

RSC Advances



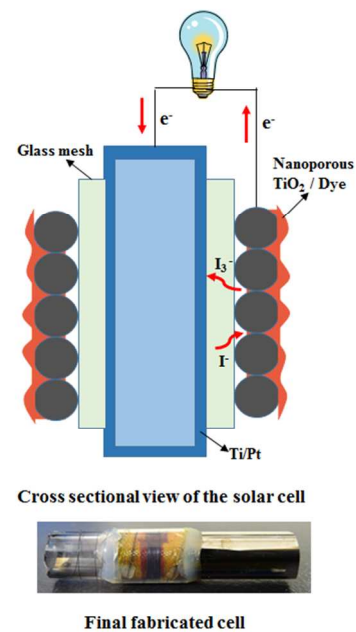
This is an *Accepted Manuscript*, which has been through the Royal Society of Chemistry peer review process and has been accepted for publication.

Accepted Manuscripts are published online shortly after acceptance, before technical editing, formatting and proof reading. Using this free service, authors can make their results available to the community, in citable form, before we publish the edited article. This *Accepted Manuscript* will be replaced by the edited, formatted and paginated article as soon as this is available.

You can find more information about *Accepted Manuscripts* in the [Information for Authors](#).

Please note that technical editing may introduce minor changes to the text and/or graphics, which may alter content. The journal's standard [Terms & Conditions](#) and the [Ethical guidelines](#) still apply. In no event shall the Royal Society of Chemistry be held responsible for any errors or omissions in this *Accepted Manuscript* or any consequences arising from the use of any information it contains.

A novel coil based cylindrical architecture for TCO-less DSSC is being reported. The steps of fabrication involved are relatively fast and easy for the mass production of DSSC. Advantages over the previous cylindrical architectures in many aspects are described. The effect of different metal wire characteristics on the solar cell performance discussed in detail. The results are supported with the electrochemical impedance spectroscopy along with the SEM image. Cell optimized in this novel device architecture gave an external power conversion efficiency of 3.88 % at AM 1.5 under simulated solar irradiation.



COMMUNICATION

Fabrication and characterization of coil type transparent conductive oxide less cylindrical dye-sensitized solar cells

Cite this: DOI: 10.1039/x0xx00000x

Received 00th January 2012,
Accepted 00th January 2012

DOI: 10.1039/x0xx00000x

www.rsc.org/

Gaurav Kapil*, Jin Ohara, Yuhei Ogomi, Shyam S. Pandey, Tingli Ma, and Shuzi Hayase*

Flexible metal wires were used to fabricate transparent conductive oxide (TCO) less cylindrical dye-sensitized solar cells (DSSCs) with very easy and fast fabrication process. Nature of the wire and interfacial contact between the metal wire and nanoporous TiO₂ layer affected the charge transport giving the photoconversion efficiency of 3.88%.

Dye-sensitized solar cells (DSSCs)^{1,2} are undoubtedly most interesting and feasible concept for developing the cost effective photovoltaic cells with the high photoconversion efficiency to meet the global energy demand^{3,4}. For industrial application point of view, cost of production and ease of fabrication are crucial issues. Conventional DSSCs utilize a transparent conducting oxide (TCO) electrode which is one of the bottlenecks towards the cost reduction.^{5,6} For the past few years, researchers have directed their efforts in fabricating TCO-less DSSC with different device architectures in a manner to match the efficiency of standard DSSCs while reducing the cost.⁷⁻¹⁰ Interest in TCO-less structure is obvious due to its advantages for fabrication in a variety of device architectures and enhanced areas of application. Apart from this, TCO-less architecture avoids losses due to optical transmission enabling it to absorb light in the near infra-red (NIR) to IR wavelength

region also. To circumvent this problem, we have reported all metal type flat DSSCs devoid of TCO completely having nearly similar photoconversion efficiency as compared to its TCO-based counterparts.⁷ Fragile nature of the TCO and restrictions on shape variations, polymer based flexible plastic electrode for the DSSCs¹¹ have also been reported recently. However, due to lack of high temperature durability of polymers, we have reported stainless-steel mesh coated with gradient TiO_x layer working as flexible working electrode.⁸ This mesh based electrode has recently been utilized in our laboratory to fabricate DSSCs in the cylindrical device architecture.¹² The cylindrical DSSC was fabricated by inserting this flexible metal mesh based photoanode, metal rod as counter electrode and porous polymer film containing electrolyte into a cylindrical glass tube. Cylindrical TCO-less DSSCs offer additional advantage over flat standard DSSC such as self-light tracking, reduced sealing and installation costs.

In the recent past, some of the works pertaining to the fabrication of DSSCs based on metallic wires have also been reported.¹³⁻¹⁶ Lu *et al*¹⁵ have reported a device structure utilizing titanium wire in the spiral shape. In this structure the large amount of electrolyte inserted may be responsible for less absorption of incident light by TiO₂ coated wire. Fuet *et al*¹⁶ have also reported the DSSCs having cylindrical architecture based on the metallic wires, however, we feel that in their architecture, the counter electrode (Pt wire) could hinder the incident light falling on to the photo electrode owing the shading effect by top catalytic and current collecting electrode. Problems pertaining to such shading effect due to counter electrode leading to reduced photon harvesting have been realized and discussed already in the recent past.¹⁷⁻¹⁹ Some researchers directed their efforts in this context with partial successes.^{15,18} However, in case of complete removal of the shading effect, other issues such as large electrolyte insertion and complex fabrication process are still the existing technical barriers.

Graduate School of Life Science and Systems Engineering,
Kyushu Institute of Technology, 2-4 Hibikino, Wakamatsu,
Kitakyushu 808-0196, Japan

E-mail: gauravkapil.ece@gmail.com,

hayase@life.kyutech.ac.jp

† Electronic Supplementary Information (ESI) available: [details of any supplementary information available should be included here]. See DOI: 10.1039/c000000x/

Keeping these pros and cons in mind, we would like to report a novel TCO-less DSSC architecture to fabricate cylindrical DSSCs based on nanoporous TiO_2 coated metal wires. The structure showed its effectiveness for roll-to-roll mass production compared to conventional and previous cylindrical DSSCs architecture reported so far. The machinery required and stages of production (such as, mount making, wire coiling, glass tube preparation, base preparation and assembly used in the incandescent lighting appliance production technology) is almost similar and can be easily adopted for the investigated coil type cylindrical architecture.

Figure 1 exhibits the schematic of the processes involved in the fabrication of coil type cylindrical DSSC. First a thin layer of titanium metal was sputtered on a cylindrical glass tube (Outer diameter, 7 mm) followed by coating of a thin Pt catalytic layer to fabricate the counter electrode. A glass mesh (20 μm thick, Asahi glass Co. Japan) was then wrapped over the counter electrode to work as spacer along with serving the purpose of holding the redox electrolyte also. The metal wires were then wrapped by coiling them around the glass mesh. Nanoporous TiO_2 D/SP (Solaronix SA) was coated over the wrapped wire. The wires utilized for the present work were (1) commercially available Ti wire ($\Phi=57\mu\text{m}$), (2) stainless steel wire (SUS-316, $\Phi=50\mu\text{m}$) and (3) Ti sputtered stainless steel wire (SUS-316, $\Phi=50\mu\text{m}$). All the metal wires used in this work were employed as received without any prior surface treatments. The thickness of the sputtered Ti was 240 nm.

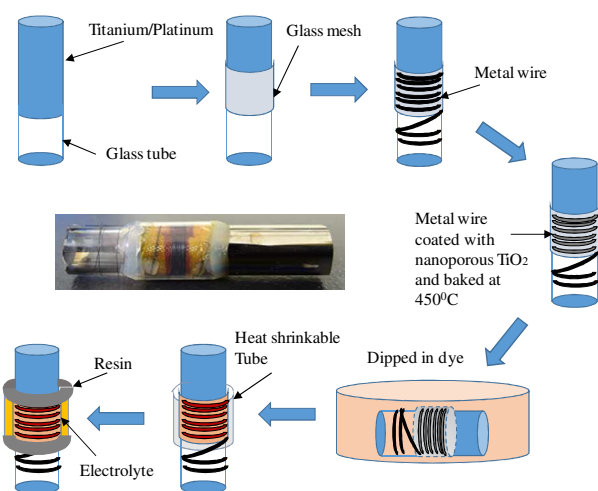


Fig. 1 Schematic representation for the fabrication of coil type TCO-less cylindrical DSSC.

The TiO_2 coated wire was gradually heated from room temperature to 450°C for 1 hour followed by sintering at this temperature for 30 min. The sintered electrode was allowed to cool down to 100°C and was subjected to sensitization with the dye cis-bis-(isothiocyanato)bis(2,2'-bipyridyl-4,4'-dicarboxylato)ruthenium(II)bis-tetrabutyl ammonium (Solaronix SA, Ruthenium 535-bisTBA abbreviated as N719) 0.3 mM in t-butyl alcohol and acetonitrile (1:1 V/V) for 24 hours at the room temperature. The structure was then covered with heat shrinkable tube ($\Phi=9.5\text{mm}$, JUNFLON NF090, Junkosha Inc.,

Japan) which shrinks to ($\Phi=7.3\text{mm}$) after heating at 120°C for 5 min. Finally electrolyte containing 50 mM iodine, 500 mM lithium iodide, 580 mM t-butylpyridine and 600 mM 1-ethyl-3-methylimidazolium dicyanoamide in acetonitrile was filled inside the heat shrinkable tube containing the whole structure and sealed at the both ends. Photovoltaic performance of the device was measured with a solar simulator (KHP-1, Bunko-Keiki, Japan) equipped with a xenon lamp (XLS-150A). The intensity of light irradiation was adjusted to AM1.5 ($100\text{mW}/\text{cm}^2$). The solar simulator spectrum and its power was adjusted using a spectroradiometer (LS-100, Eiko Seiki, Japan). The exposure power was also corrected with standard amorphous Si photo detector (BS-520 S/N 007, Bunko-Keiki, Japan), which has similar visible light sensitivity to the DSSC. The irradiation area of the device was calculated by multiplying the width of the wire wrapped with the diameter of the counter electrode. The device characteristics were measured without any mask and whole device was exposed to the simulated light source. Photocurrent action spectrum also known as incident photon conversion efficiency as function of wavelength for the devices prepared were measured with a constant photon flux of 1×10^{16} photon/ cm^2 at each wavelength in the direct current mode using the action spectrum measurement system connected to the solar simulator (CEP-2000, Bunko Keiki, Japan). Electrochemical impedance spectroscopy (EIS) measurements were also carried out with a frequency response analyser (Solartron Analytical, 1255B) connected to a potentiostat (Solartron Analytical, 1287) under illumination of $100\text{mW}/\text{cm}^2$ light using a Yamashita Denso YSS-50A solar simulator. EIS measurements were performed in the frequency range of 5×10^{-3} – 10^5 Hz at room temperature. The electrical impedance spectra were characterized using Z-View software (Solartron Analytical). The thickness of the nanoporous TiO_2 film coated on the different metal wire was estimated by taking the cross-sectional image using scanning electron microscope (JEOL, NeoScope JCM-6000).

Figure 2a shows schematic cross-sectional view of the device architecture. Typically, its working principle is similar to the conventional DSSC. Dye molecules adsorbed over the nanoporous TiO_2 harvests the photons. Photoexcited dye molecules inject electrons into the conduction band of the TiO_2 layer. Electrons are then transported towards the metal wire and the external circuit to counter electrode (Ti/Pt). The oxidized dye is then reduced by I^- present in the glass mesh soaked with electrolyte and this I^- is reproduced by the reduction of I_3^- with electrons from counter electrode (Ti/Pt). Figure 2b exhibits the scanning electron microscopic (SEM) image for the cross-sectional view of the photoanode which was taken in order to determine the thickness of the nanoporous TiO_2 layer coated on to the metal wire. Relatively less contrasting nanoporous TiO_2 layer can be clearly seen which is mainly coated on the top of the metal wires and the spacing between the wires. At the same time, average thickness of this nanoporous TiO_2 layer was found to be approximately $10\mu\text{m}$.

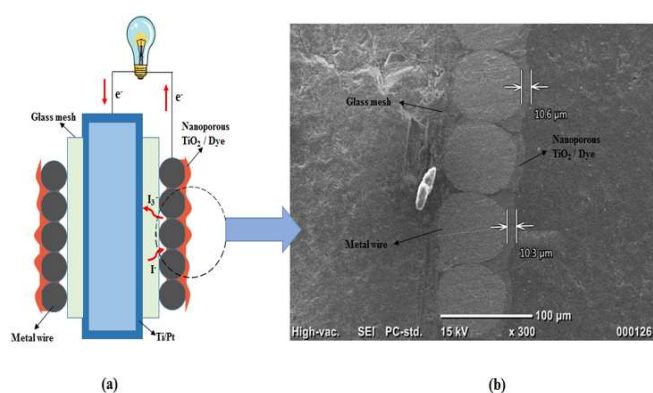


Fig. 2 (a) Schematic cross-sectional view of the device. (b) Scanning electron microscope image of nanoporous TiO₂ coated metal wire.

Figure 3 shows photovoltaic performance of the coil based TCO-less cylindrical solar cells fabricated using different metal wires utilized for the fabrication of the photoanode along with the photovoltaic parameters shown in the Table 1. This figure and Table 1 clearly indicate that nature of the wire plays an important role towards controlling the overall photoconversion efficiency of the device. Photoconversion efficiencies (η) were found to be in the order Ti < SS-Steel (SS) < Ti-sputtered Stainless steel (SS/Ti) wires. A remarkable enhancement in the photoconversion efficiency was observed for photoanode based on SS/Ti wires as compared to the cylindrical DSSCs fabricated using SS and Ti wire based photoanodes. This tremendous increase in the overall photoconversion efficiency of coil based cylindrical DSSC using SS/Ti was resulting from enhancement in the all of the photovoltaic parameters such as open circuit voltage (Voc), short circuit current density (Jsc) and fill factor (FF) as shown in the Table 1.

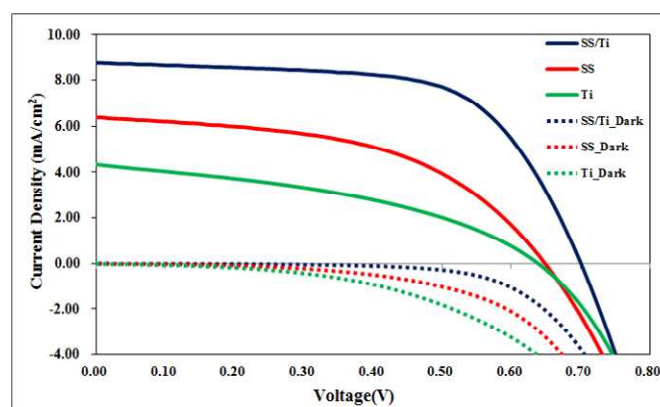


Fig. 3 Photo/dark current-voltage characteristic for DSSCs using different metal wires.

Under simulated AM 1.5 solar irradiation, this SS/Ti wire based DSSC exhibited a Jsc of 8.75 mA/cm² with much improved FF of 0.63 and an enhanced Voc of 0.70 V resulting in to the overall photoconversion efficiency of 3.88%. On the other hand Ti wire exhibited the poorest photovoltaic performance ($\eta=1.12\%$) which was highly affected by the drastically

hampered both of the Jsc and FF. Another striking difference can be noticed that photoanodes based on Ti and SS wires, the observed dark currents are much higher as compared to the photoanode based on SS/Ti wires. Therefore, this hampered dark current for SS/Ti could be attributed to the observation of higher Voc due to suppressed charge recombination. Thus sputtering of titanium over the stainless steel wire could be the possible reason for the reduced charge recombination as titanium coating forms a charge recombination blocking layer⁸.

Table-1 Photovoltaic and EIS parameters for metal wire based TCO-less cylindrical solar cells under simulated solar irradiation.

Parameters	SS	SS/Ti	Ti
Efficiency (%)	2.09	3.88	1.12
FF	0.50	0.63	0.40
Voc [V]	0.65	0.70	0.64
Jsc [mA/cm ²]	6.38	8.75	4.35
R1 (Ω)	35.47	36.43	25.97
R2 (Ω)	100.2	88.38	56.43
R3 (Ω)	391.2	188.1	2433
Dye loading amount [nmol/cm ²]	319.4	318.6	322.6

Since Jsc is one of major controlling factors of the overall photoconversion efficiency of our coil based cylindrical DSSCs with the nature of metal wires under investigation, spectral response of the DSSCs were also measured to elucidate this observed differential behaviour. Figure 4 depicts the incident photon-to-current conversion efficiency (IPCE) as a function of wavelength. It can be clearly seen that DSSC based on SS/Ti wire exhibits the highest IPCE (48 %) at around 550 nm (absorption maximum of N-719 on TiO₂ surface) supports the highest observed Jsc in the J-V curve as compared to DSSCs based on other wires. Lack of photon harvesting in the 300-400 nm wavelength region could be attributed to the available electrolyte layer between the heat shrinkable tube and photoanode is still large enough to absorb the appreciable amount of light by the electrolyte layer itself. Such kind of observation has also been made and reported by our group previously for the TCO-less cylindrical DSSCs based SS-mesh¹². The possibility of difference in IPCE could also be argued due to different extent of the dye loading on different metal wire surfaces coated with nanoporous TiO₂. To check the validity of this reason, the amount of dye loading was also estimated using equal volume of NaOH (0.1M) solutions of ethanol, t-butyl alcohol and acetonitrile as dye desorption solvent. The results pertaining to estimation of the extent of dye molecules shown in Table 1 strictly ruled out this possibility as it shows approximately same amount of dye loading for all of the three metal wire based photoanodes.

In order to understand observed differential photovoltaic behaviour for the photoanodes based on different metal wires particularly Jsc, EIS measurements were also conducted to investigate the interfacial charge transfer processes. To analyse the EIS spectra, adequate physical models and suitable equivalent circuits have been proposed and widely implemented to study interfacial electron transfer processes in

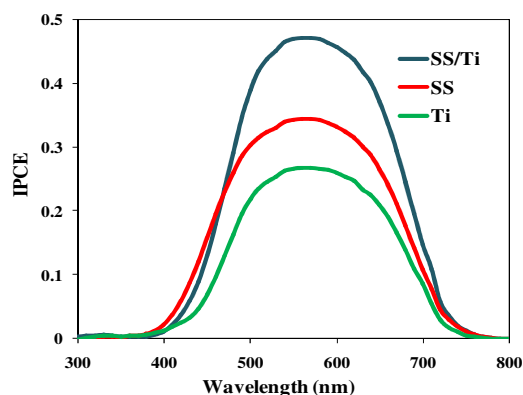


Fig. 4 Incident photon-to-current conversion efficiency (IPCE) curves for TCO-less coil based DSSCs using different metal wires.

DSSCs.²⁰⁻²⁴ Figure 5 exhibits the plot of real vs. imaginary part of the complex impedances (Nyquist plot) measured under AM 1.5 condition light illumination at constant J_{sc} of 1 mA/cm^2 . First impedance element (R1) in the high frequency region is attributed to the series resistance of the conducting layer such as metal wires in the present case which do not show appreciable differences. The resistance associated with first semi-circle (R2) is assigned to the charge transfer at the counter electrode, which was not an important factor for the different behaviour of the solar cell performance. The second semi-circle appearing in the mid frequency region is attributed to be originated from the charge-transfer resistance (R3) of working electrode/ TiO_2 and TiO_2 /electrolyte interfaces. There are two possible interpretations for the origin of this semi-circle.²⁵ First is related to the proper electrical contact between the metal wire and TiO_2 nanoparticle while second interpretation is associated with charge recombination between TiO_2 and electrolyte.^{23,25}

The most striking differences in the resistance for this second semi-circle was observed for the photoanodes using different metal wires in the present investigation. SS/Ti shows very small resistance ($188\ \Omega$) in this region as compared to Ti wire ($2433\ \Omega$) which can be explained by enhanced interfacial adhesion between working electrode and nanoporous TiO_2 . This facilitates the facile electron transport resulting into improved photovoltaic performance. The second possibility of large recombination resistance for Ti in our case can be ruled out since it shows relatively small J_{sc} and V_{oc} as compared to the SS/Ti. The differential behaviour observed for photoanodes based on Ti and SS/Ti wires can be explained by the presence of different extents of TiO_x surface defects on the commercial Ti wire which might be passivated by sputtering of pure titanium on the stainless steel wire (SS/Ti) and are supposed to hinder the better contact between the metal wire and nanoporous TiO_2 . Similar enhancement in the electrical contact formation between the substrate and nanoporous TiO_2 by different kinds of surface treatments of metal foil for TiO_x surface passivation resulting into improved photovoltaic performance has also been advocated by A. Jiang et al.²⁶

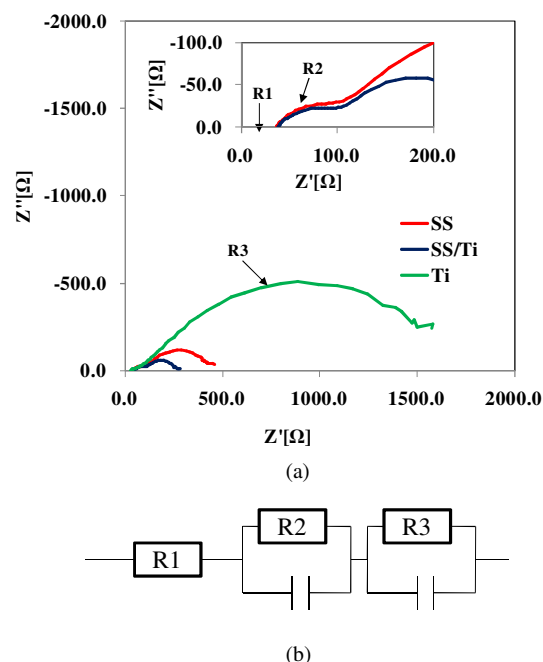


Fig. 5(a) EIS spectra of coil based TCO-less DSSCs measured at AM1.5 and constant J_{sc} of 1 mA/cm^2 and **(b)** Electrical equivalent circuit for impedance spectra.

In conclusion, we fabricated a novel TCO-less cylindrical dye-sensitized solar cell with more ease and fast method of fabrication compared to other TCO-less DSSC architectures. Problems related to previous device architectures such as shading effect and complex fabrication process were minimized. It has been demonstrated that nature of wire and surface treatment plays an important role in controlling the device performance. EIS investigation revealed that in spite of charge recombination between TiO_2 /Dye/Electrolyte interface, better electrical contact between metal wires and nanoporous TiO_2 plays a dominating role in controlling the overall photovoltaic performance. Coating of thin pure Ti metal over SS wire as surface passivating and electron recombination blocking layer led to the dramatic enhancement in the photoconversion efficiency from 1.12 % (Ti) to 3.88% (SS/Ti).

References

- 1 M. Grätzel, *Nature*, 2001, 414, 338.
- 2 A. Hagfeldt and M. Grätzel, *Acc. Chem. Res.* 2000, 33, 269.
- 3 B. O'Regan and M. Grätzel, *Nature*, 1991, 353, 737.
- 4 M. Grätzel, *Inorganic Chemistry*, 2005, 44, 6841.
- 5 M. Grätzel, *Acc. Chem. Res.* 2009, 42, 1788.
- 6 J.M. Kroon, N.J. Bakker, H.J.P. Smidt, P. Liska, K.R. Thampi, P. Wang, S.M. Zakeeruddin, M. Grätzel, A. Hinsch, S. Hore, U. Würfel, R. Sastrawan, J.R. Durrant, E. Palomares, H. Pettersson, T. Gruszeczi, J. Walter, K. Skupien and G.E. Tulloch, *Prog. Photo: Res.App.*, 2007, 15, 1.
- 7 Y. Kashiwa, Y. Yoshida and S. Hayase, *App. Phys. Lett.*, 2008, 92, 033308.

- 8Y. Yoshida, S.S. Pandey, K. Uzaki, S. Hayase, M. Kono and Y. Yamaguchi, *App. Phy. Lett.*, 2009, 94, 093301.
- 9N. Fuke, A. Fukui, R. Komiya, A. Islam, Y. Chiba, M. Yanagida, R. Yamanaka and L. Han, *Chem. Mat.*, 2008, 20, 4974.
- 10T. Beppu, Y. Kashiwa, S. Hayase, M. Kono and Y. Yamaguchi, *Jap. J.App.Phy.*, 2009, 48, 061504.
- 11T. Miyaska and Y. Kijitori, *J.Electrochem. Society*, 2004, 151, A1767.
- 12J. Usagawa, S.S. Pandey, Y. Ogomi, S. Noguchi, Y. Yamaguchi and S. Hayase, *Prog.Photo.:Res. App.*, 2013, 21, 517.
- 13X. Fan, Z. Chu, F. Wang, C. Zhang, L. Chen, Y. Tang and D. Zou, *Adv. Mat.*, 2008, 20, 592.
- 14J. Yu, D. Wang, Y. Huang, X. Fan, X. Tang, C. Gao, J. Li, D. Zou and K. Wu, *Nano. Res. Lett.*, 2011, 6, 94.
- 15Y. Liu, H. Wang, H. Shen and W. Chen, *App. Energy*, 2010, 87, 436.
- 16Y. Fu, Z. Lv, H. Wu, S. Hou, X. Cai, D. Wang and D. Zou, *Sol. Energy Mater. Sol. Cells*, 2012, 102, 212.
- 17Z. Liu and M. Misra, *ACS Nano*, 2010, 4, 2196.
- 18Y. Wang, Y. Liu, H. Yang, H. Wang, H. Shen, M. Li, and J. Yan, *Curr. Appl. Phys.*, 2010, 10, 119.
- 19L. Sun, S. Zhang and Q. Wang, *Journal of Nano Sci. & Tech.*, 2014, 14, 2064.
- 20F. Fabregat-Santiago, J. Bisquert, E. Palomares, L. Otero, D. Kuang, S.M. Zakeeruddin and M. Grätzel, *J. Phys. Chem. C*, 2007, 111, 6550.
- 21R. Kern, R. Sastrawan, J. Ferber, R. Stangl, J. Luther, *Electrochim. Acta*, 2002, 47, 4213.
- 22Y. Yoshida, S. Tokashiki, K. Kubota, R. Shiratuchi, Y. Yamaguchi, M. Kono and S. Hayase, *Sol. Energy Mater. Sol. Cells*, 2008, 92, 646.
- 23H. Choi, C. Nahm, J. Kim, J. Moon, S. Nam, D.R. Jung and B. Park, *Current App. Phy.*, 2012, 12, 737.
- 24Q. Wang, J.E. Moser and M. Grätzel, *J. Phy. Chem. B*, 2005, 109, 14945.
- 25M. Kim, I.K. You, K.W. Lee, I.H. Lee and H.G. Yun, *App. Phy. Lett.*, 2013, 102, 183904.
- 26J. An, W. Guo and T. Ma, *Small*, 2012, 8, 3427.